Gallium Nitride Materials—Progress, Status, and Potential Roadblocks

ROBERT F. DAVIS, AMY M. ROSKOWSKI, EDWARD A. PREBLE, JAMES S. SPECK, BEN HEYING, JAIME A. FREITAS, Jr., EVAN R. GLASER, AND WILLIAM E. CARLOS

Invited Paper

Metal–organic vapor phase epitaxy (MOVPE) and molecular beam epitaxy (MBE) are the principal techniques for the growth and n-type (Si) and p-type (Mg) doping of III-nitride thin films on sapphire and silicon carbide substrates as well as previously grown GaN films. Lateral and pendeoepitaxy via MOVPE reduce significantly the dislocation density and residual strain in GaN and AlGaN films. However, tilt and coalescence boundaries are produced in the laterally growing material. Very high electron mobilities in the nitrides have been realized in radio-frequency plasma-assisted MBE GaN films and in two-dimensional electron gases in the AlGaN/GaN system grown on MOVPE-derived GaN substrates at the crossover from the intermediate growth regime to the droplet regime. State-of-the-art Mg doping profiles and transport properties have been achieved in MBE-derived p-type GaN. The Mg-memory effect, and heterogeneous growth, substrate uniformity, and flux control are significant challenges for MOVPE and MBE, respectively. Photoluminescence (PL) of MOVPE-derived unintentionally doped (UID) heteroepitaxial GaN films show sharp lines near 3.478 eV due to recombination processes associated with the annihilation of free-excitons (FEs) and excitons bound to a neutral shallow donor (D^oX). All six allowed Raman modes were observed with small full-width at half-maximum values. The introduction of Si or Mg introduces an intense edge emission assigned to a recombination process associated with X-Si^o or a deep compensating donor, respectively. The PL spectrum of hydride-vapor-phase-epitaxy-derived freestanding GaN templates showed, within the 3.46–3.52-eV region, emission lines assigned to the excited state of the FE A (FX_A^1) and the dominant D^oX. Significant concentrations of Si and O donors were revealed by Fourier transform infrared and secondary ion mass spectrometry studies of UID freestanding samples. The results of magnetic resonance studies of shallow donors and acceptors, the 2.2-eV "yellow" PL band, and defects created by electron irradiation of native defects and dopants in GaN and/or AlGaN are detailed.

Keywords*—Aluminum gallium nitride (AlGaN), defects, dislocations, dopants, electron irradiation, electron mobilities, excitons, Fourier transform infrared (FTIR) absorption, gallium nitride (GaN), heteroepitaxy, hydride vapor phase epitaxy (HVPE), lateral epitaxial overgrowth, magnetic resonance, metal–organic vapor phase epitaxy (MOVPE), Mg doping, molecular beam epitaxy (MBE), pendeoepitaxy, photoluminescence, Raman spectroscopy, recombinations, secondary ion mass spectrometry (SIMS), Si doping, two-dimensional electron gas.*

Manuscript received October 14, 2001; revised February 15, 2002. This work was supported in part by the Office of Naval Research under Contract N00014-98-1-0654 and Contract N00014-99-1-0729 and in part by the Naval Research Laboratory. The work of R. F. Davis was supported in part by Kobe Steel, Ltd.

R. F. Davis and E. A. Preble are with the Department of Materials Science and Engineering, North Carolina State University, Raleigh, NC 27695-7907 USA (e-mail: Robert_Davis@ncsu.edu; epreble@datatrendsoftware.com).

A. M. Roskowski is with the Intel Corporation, Portland, OR 97124 USA (e-mail: amy@unifusion.com).

J. S. Speck is with the Materials Department, University of California, Santa Barbara, CA 93106 USA (e-mail: speck@mrl.ucsb.edu).

B. Heying is with the TRW Corporation, Redondo Beach, CA 90278-1071 USA (e-mail: Benjamin.Heying@trw.com).

J. A. Freitas, Jr., E. R. Glaser, and W. E. Carlos are with the Naval Research Laboratory, Washington, DC 20375-5347 USA (jaime.freitas@nrl.navy.mil; glaser@bloch.nrl.navy.mil; Carlos@bloch.nrl.navy.mil).

Publisher Item Identifier S 0018-9219(02)05575-5.

I. Metal–Organic Vapor Phase Epitaxy of III-Nitride Films

A. Overview of Technique and Its Application to III-Nitrides

Chemical vapor deposition (CVD) is the generic name for processes that involve a dynamic flow system in which gaseous reactants pass over a heated substrate and react to form a condensed layer or film on the substrate. Metal–organic vapor phase epitaxy (MOVPE) is one of the forms of CVD that is used for the growth of thin films of (Al, In, Ga)N binary compounds and solid solutions. Several sequential process steps may be applicable in the growth of these materials, e.g., adduct formation in the gas phase [1], adsorption, decomposition, and diffusion and reaction on the existing surface between Group III metal–organic precursors, e.g., triethylgallium or trimethylgallium, trimethylaluminum and trimethylindium, and NH_3. A large V(NH_3)/III (metal–organics) gas ratio is used to offset the loss of nitrogen due to surface decomposition. Either hydrogen or nitrogen is used as the diluent to prevent homogeneous nucleation of solid particles in the gas phase. The MOVPE system is operated in a mass-transport limited-growth regime during the growth of III-nitride films, i.e., the growth rate of the film is dependent

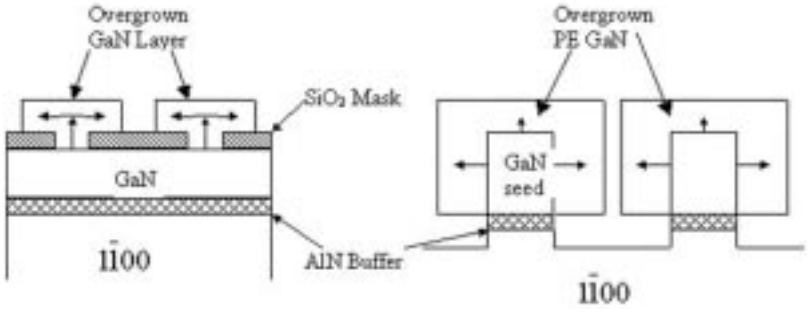

Fig. 1. Schematic of (a) LEO growth through a window in SiO_2 and laterally over the mask. (b) PE growth from GaN seed laterally off the sidewalls and vertically off the stripe.

on the transport of the reactant gases to the surface and layer composition and uniformity are controlled by the reactor geometry and flow conditions.

A complete range of solid solutions can be deposited from pure GaN to pure AlN at substrate temperatures exceeding 1000 °C. By contrast, only ∼30% In can be incorporated (essentially "captured") into an MOVPE-grown GaN-based alloy prior to the onset of phase separation [2], [3]. Increasing the growth rate and the use of a nitrogen diluent increases the concentration of InN incorporated into a film at a given temperature [4]–[6]. Growth temperatures <800 °C are normally used.

B. Recent Advances in the MOVPE of GaN and AlGaN

Growth of thin films of GaN and selected AlGaN alloys have cleared three major hurdles: 1) heteroepitaxy, i.e., the epitaxial growth of a layer on a substrate or another layer having a different chemical composition and/or crystallography via the use of intermediate GaN, AlN or AlGaN buffer layers [7]–[9]; 2) control of donor (n-type) and acceptor (p-type) doping with Si and Mg, respectively; and 3) a marked reduction in the dislocation density. The high residual electron concentrations in the early samples of GaN were almost universally attributed to the donor character of nitrogen vacancies. However, first-principles calculations by Van de Walle [10] showed that the energy of formation of nitrogen vacancies is too high for their incorporation in GaN during growth, but oxygen and silicon readily form donors. This theory has received experimental support as a result of: 1) the decrease/increase in the carrier concentration/mobility of undoped GaN following the development of high-purity ammonia sources having <200 ppb H_2O levels and 2) the controlled increase in the n-type carrier concentration without compensation via the measured introduction of oxygen with a 33-MeV donor energy level into a GaN film in an extremely clean growth environment via molecular beam epitaxy (MBE) [11]. The results of additional MBE studies are presented below.

The aforementioned high intrinsic donor concentration was an impediment, but not the only problem, in the achievement of p-type conductivity. More recent research showed that a postgrowth exposure to an electron beam [12] or thermal annealing in nitrogen [13] was needed to activate and ionize acceptor dopants, e.g., Mg, to achieve p-type GaN grown via MOVPE. It was subsequently determined [14], [15] that the growth in the presence of hydrogen results in the formation Mg–H complexes on the growing surface that become incorporated into the film. Heating dissociates these complexes, but the H does not evaporate. A third problem in p-type doping in MOVPE reactors is the "Mg memory" effect that leads to very broad doping profiles, making careful p-n junction placement difficult. Donor (Si) and acceptor (Mg) doping and corresponding electrical behavior have also been achieved in AlGaN alloys to maximum AlN concentrations of ∼58% and ∼13%, respectively [16].

Essentially, all films of III-Nitride materials are heteroepitaxially grown on sapphire [α–Al_2O_3(0001)] or silicon carbide [SiC(0001)]. These substrates have lattice parameters and coefficients of thermal expansion that are, respectively, +16% and +39% (sapphire) and −3.5% and −3.2% (SiC), relative to GaN. The residual stresses caused by these mismatches are accommodated by the formation of misfit and threading dislocations, the latter of which occur throughout thin films in densities of $\sim 10^9$ cm^{-2}. Edge and mixed (screw/edge) dislocations in GaN: 1) are nonradiative recombination centers [17]; 2) act as conduits for charge transport, which results in high leakage currents and slow breakdown of rectifying contacts; and 3) reduce significantly the lifetime of laser diodes. By comparison, dislocation densities in "bulk" GaN single crystals and MOVPE films grown on them are reported to be $\leq 10^4$ cm^{-2} [18]. The latter also exhibit on-axis full-width at half-maximum (FWHM) values of X-ray diffraction rocking curves of 20 arcsec donor-bound exciton (D^oX) linewidth of 114 μeV and an acceptor-bound exciton (A^oX) linewidth of 95 μeV [18]. These values are an order of magnitude lower than the best MOVPE lateral epitaxial overgrowth (LEO) GaN on sapphire [19], [20]. Unfortunately, the limited availability and small size of these crystals have restricted their use.

Many research groups have shown that LEO can reduce the dislocation density in GaN films grown by MOVPE. Early reports of the achievement of material having a low density of dislocations via lateral overgrowth by Nam *et al.* [21] and the success of Nakamura *et al.* [22] in the fabrication of a GaN-based blue light-emitting laser diode with a lifetime over 10 000 h grown on LEO material have spurred considerable attention to overgrowth techniques. LEO involves the patterning of a SiO_2 mask on a GaN film with stripe windows in the mask. The selectively deposited material grows vertically to the top of the mask and laterally over the mask, as shown in Fig. 1(a). The

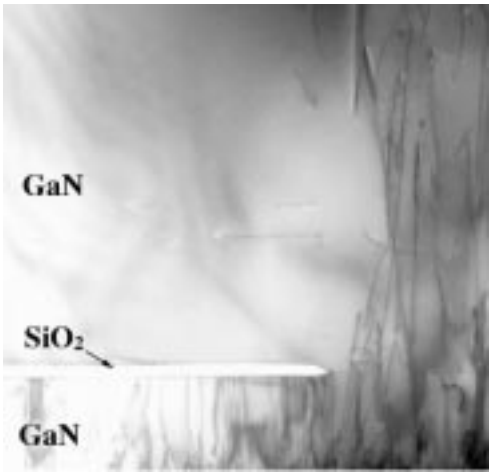

(a)

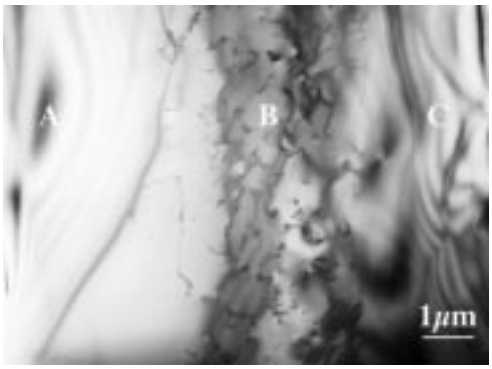

(b)

Fig. 2. (a) Cross-sectional TEM micrograph from a stripe along the $[11\bar{2}0]$ direction. Two distinct regions of high-defect density above the window and of nearly defect-free GaN above the SiO_2 are clearly visible. (b) Plan view TEM from a GaN stripe. Region A and C correspond to areas over the SiO_2 and are nearly defect-free. Region B corresponds to the area over the window with a dislocation density of $8 \times 10^8 - 4 \times 10^9$ cm^{-2}.

density of threading dislocations in the laterally overgrown layer is markedly reduced, as evidenced by the transmission electron microscopy (TEM) micrographs shown in Fig. 2 [23]. Pendeoepitaxy (PE) is another overgrowth technique in which GaN seed stripes are etched into the SiC substrate and GaN or AlGaN is regrown laterally and vertically off the stripe regions, as shown in Fig. 1(b). The dislocation density in the laterally grown sidewall regions is reduced by at least four orders of magnitude relative to the 10^9 cm^{-2} density in the initial GaN seed layer, as shown in the $Al_{0.1}Ga_{0.9}N$ film in Fig. 3 [24], [25].

PE incorporates mechanisms of growth exploited by conventional LEO processes with one main advantage, the elimination of the growth mask. Conventional LEO employs a SiO_2 or SiN mask to stop the vertical propagations of defects into the overgrown material [21]. In PE, GaN selectively grows only off the etched GaN seed, as the substrate acts as a pseudomask and the overgrowth region coalesces and is suspended above the substrate [see Fig. 3(a)]. The elimination of a growth mask has three main advantages.

1) Crystallographic tilt in the overgrown material is significantly reduced. Tilt results in crystallographic misregistry and boundary formation at the region of coalescence [25], [26].
2) Diffusion of impurities from the mask into the overgrowth material increases the background donor concentration two orders of magnitude in LEO material [27]; carrier concentrations in PE remain below 1E17 cm^{-3}.
3) AlGaN alloys nucleate on mask materials and PE provides a means for growth of low-defect AlGaN films that cannot be accomplished with LEO [28].

Fig. 3. Composite of cross-sectional TEM micrographs of a PE $Al_{0.1}Ga_{0.9}N$ film. Note the threading dislocations continue from the GaN stripes into the film.

Measurement of strain in GaN films grown via PE indicates that the overgrowth or wing material is crystallographically relaxed. The presence of screw- and edge-type dislocations in the stripe and wing areas were determined via ω scans of the (0002) and $(30\bar{3}2)$ X-ray reflections, as described in [29]. The FWHM values of the rocking curves in the on-axis (0002) reflection compare the concentration of screw-type dislocations while comparisons of off-axis $(30\bar{3}2)$ FWHM values determine the relative density of edge-type dislocations. Reciprocal space maps of the uncoalesced PE material show a center peak produced by the seed material and two side peaks produced by the two wings when the beam direction is perpendicular to the seed stripe direction. A reduction in screw-type dislocations in the wings with respect to the stripes is indicated by a reduction in FWHM of the (0002) reflections from 646 arcsec to 354 arcsec. The off-axis FWHM of the wing area was 126 arcsec compared to 296 arcsec for the stripe, indicating a reduction in the edge type dislocations as well.

The two wing peaks are shifted with respect to the seed layer peak in both the omega direction and the 2θ–ω direction. The omega shift is produced by crystal tilt in the wing regions ($\sim$0.15°) and the 2θ–ω shift is due to strain relaxation in the wing regions. Once free of the strain effects of the substrate, a slight relaxation of both the a($-$0.07%) and c($+$0.03%) lattice parameters was observed in the wing region. An upward shift of the E2 Raman line of approximately 0.7 wave numbers in the wing area with respect to the stripe was observed and indicated a relaxation in the former. A change in the c-axis lattice parameter of $\sim$0.02% was calculated from the frequency shift [30] and agrees well with the calculated change in c-axis measured with X-ray diffraction. The wing material is relaxed with less strain and also emits very sharply in photoluminescence (PL). The donor-bound exciton emission peak in the wing material is very sharp

with a FWHM value less than 300 μeV (below the resolution of the equipment) and is comparable to homoepitaxy GaN grown on bulk GaN crystals [19]. PE growth of wings off the $(11\bar{2}0)$ surface of a GaN stripe produces a material that is crystallographically relaxed, contains fewer defects compared to the stripe, and is atomically smooth on the $(11\bar{2}0)$ surface [31].

Recently, considerable achievements in the homoepitaxial growth and doping of GaN thin films and microelectronic device structures on MOVPE-derived GaN films via MBE have been reported. As such, this technique is becoming competitive with MOVPE in some areas for the growth of III-nitrides. The following section details the recent progress and scientific understanding in this arena.

II. Progress in the Molecular Beam Epitaxy of GaN and Its Alloys

The growth of thin films by MBE occurs via reactions between thermal-energy molecular, atomic, or ionized beams of the constituent elements on a heated substrate in ultrahigh vacuum. The film composition depends on the relative arrival rates of the constituent elements that, in turn, depend on the evaporation rates or flow rates of the sources. The growth rate of the film is typically one monolayer per second. Mechanical shutters in front of the beam sources are used to interrupt the beam fluxes and, therefore, start and stop the deposition. Changes in composition can, thus, be abrupt on an atomic scale.

Homoepitaxial growth of GaN by MBE on 1–2-μm-thick GaN "template" layers deposited via MOVPE on either sapphire or Si substrates has been investigated at the University of California at Santa Barbara (UCSB) [32] in collaboration with investigators at Infineon. The templates and the 0.2–0.5-μm-thick MBE films have Ga polarity and threading dislocation densities in the mid-10^8–10^9 cm^{-2} range [33]. Growth diagrams have been instrumental in MBE growth [34], [35]. A regime within a diagram defines a set of growth conditions, i.e., group-III/group-V ratio versus substrate temperature that produces similar surface properties. Films grown under conditions that produce the same surface structure have been found to have similar properties [34], [35]. As such, these diagrams can be used to identify optimum growth regimes.

The characteristics of GaN surfaces have been studied by reflection high-energy electron diffraction (RHEED) surface reconstructions, atomic force microscopy (AFM), and scanning tunneling microscopy (STM) as a function of growth parameters. There seems to be a universal dependence of the surface morphology on the Ga/N ratio. Several groups [23], [36]–[39] have reported an abrupt transition in surface morphology between films grown under Ga-stable conditions (high Ga/N ratio) and those grown under N-stable conditions (low Ga/N ratios). Under N-stable conditions, films generally have spotty RHEED patterns and rough faceted morphologies. Ga-stable conditions (high Ga/N ratio) generally produce films having streaky RHEED patterns with smooth two-dimensional (2-D) growth morphologies. Ga-droplet formation has been found

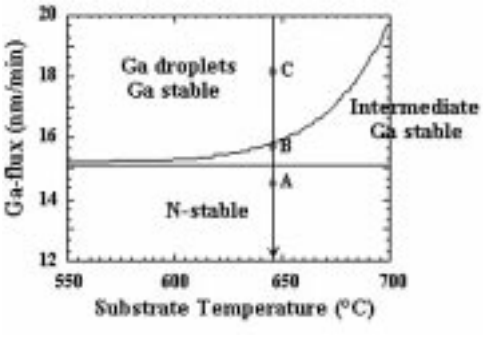

(a)

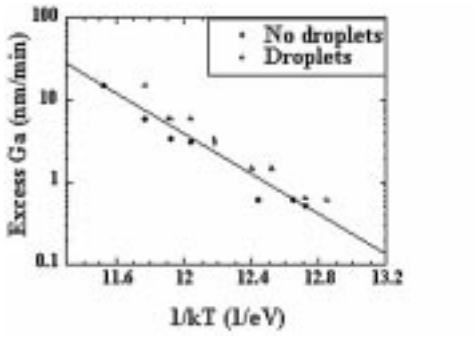

(b)

Fig. 4. (a) Surface structure diagram defining the Ga-flux conditions and substrate temperatures for the Ga droplet, intermediate, and N-stable growth regimes at a constant N flux of 15.2 nm/min. The closed circles, labeled A, B, and C, refer to the growth conditions of the samples shown in the AFM and TEM images. (b) Plot of excess Ga versus 1/kT, where the parameter excess Ga $= F^{*}_{\mathrm{Ga}} - F^{\mathrm{N}}_{\mathrm{available}}$. ($F^{*}_{\mathrm{Ga}}$ is the Ga flux and $F^{\mathrm{N}}_{\mathrm{available}}$ is the active nitrogen flux that gives rise to growth). The line was fit between the samples exhibiting droplets after growth and those that did not have droplets.

to accompany Ga-stable growth under conditions of high Ga/N ratios and low substrate temperatures [32], [37], [40].

The results of studies at UCSB [41] have defined three MBE growth regimes for GaN. The growth diagram shown in Fig. 4 depicts the Ga-flux conditions and substrate temperatures that define these growth regimes at a constant N flux. Films grown with streaky RHEED patterns that exhibit Ga droplets characterize the "Ga-droplet" regime. These films were observed at low temperatures and high Ga fluxes. Films grown with streaky RHEED patterns that did not have Ga droplets were observed at high temperatures and intermediate Ga fluxes and occurred in the "intermediate" regime. The "N-stable" regime, characterized by films having spotty RHEED patterns, was observed at low Ga fluxes for all temperatures.

The boundary between the N-stable regime and the Ga-stable regime, shown in Fig. 4(a), was determined by the growth rate of the Ga-stable films. The Ga flux was equal to the available N flux. Below this line, the growth is Ga deficient and the Ga flux limits the growth rate [39]. At fluxes above this line, excess Ga is present on the surface and the growth rate was limited by the amount of available nitrogen. Therefore, the growth rate of the films grown under Ga-stable conditions determines the amount of available N flux and, hence, the boundary shown in Fig. 4(a). This

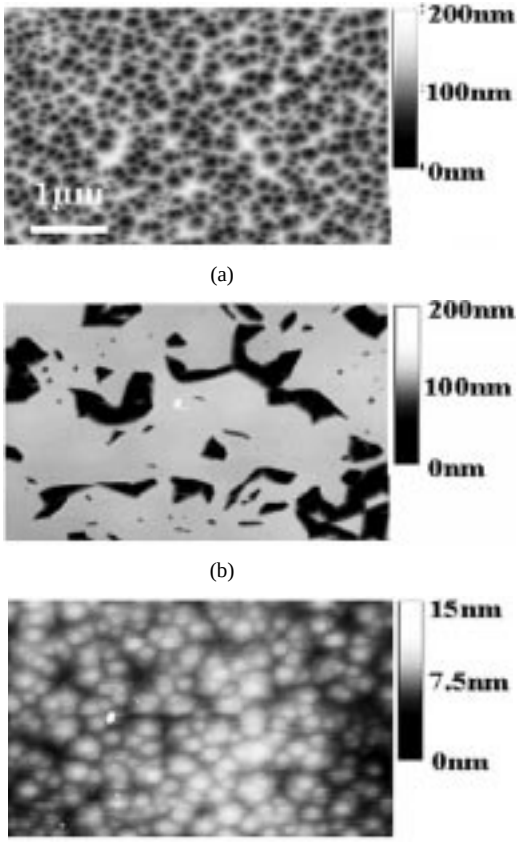

Fig. 5. AFM images of GaN samples grown within the (a) N-stable regime (Ga flux = 14.5 nm/min), (b) intermediate regime (Ga flux = 15.8 nm/min), and (c) Ga droplet regime (Ga flux = 18.2 nm/min).

boundary corresponds to the aforementioned transition between spotty and streaky RHEED patterns. This boundary is constant for all temperatures within the diagram because no temperature dependence was observed in the growth rate of Ga-stable films or N-stable films to at least 700 °C.

Growing films under various fluxes and temperatures and subsequently observing whether droplets formed during growth determined the boundary between the intermediate growth regime and the Ga-droplet growth regime. The curve shown in Fig. 4(b) was fit between the samples exhibiting droplets and those that did not. It had an Arrhenius dependence with activation energy of 2.832 eV, which corresponds to the activation energy for desorption of Ga from liquid Ga.

Films grown within the N-stable regime have a very rough crater-like morphology, as shown in Fig. 5(a). The surface of the films grown within the intermediate Ga-stable regime [see Fig. 5(b)] have large areas of uniform flat surface between pits with irregular faceted edges. The film grown within the Ga droplet regime [see Fig. 5(c)] shows no pit features and has a uniform atomically flat surface. The mottled appearance of the surfaces grown in the Ga-stable regime is caused by spiral growth about threading dislocations with mixed character. TEM studies on the last samples revealed that the pit features shown in Fig. 5(b) were associated with inclined facets that form at threading dislocations. These facets typically are $\{10\bar{1}3\}$ or $\{10\bar{1}4\}$ planes and are the

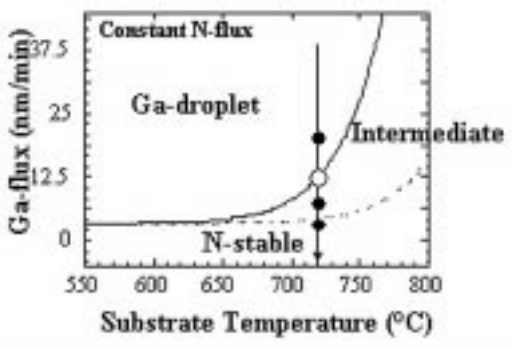

Fig. 6. Growth diagram defining the Ga-flux conditions and substrate temperatures for the Ga droplet, intermediate, and N-stable growth regimes at a constant N flux of 2.8 nm/min. Circles define the conditions used for transport studies for n-type GaN.

Table 1
RT Mobilities and Carrier Concentrations in Samples Grown Under the Conditions Signified by the Circles Shown in Fig. 6

Growth regime	Thickness (μm)	Mobility (cm^2/Vs)	Carrier conc. ($x10^{16}$ cm^{-3})
Ga-droplet	0.5	785	2.1
Ga-droplet	1.0	885	3.0
Intermediate	1.0	1100	3.2
Intermediate	0.5	845	1.2
N-stable	0.5	insulating	insulating

MBE equivalent to the common $\{10\bar{1}1\}$ facets observed in MOVPE GaN films.

Room-temperature (RT) transport studies were conducted at UCSB [42] on films grown at a constant substrate temperature within the range of Ga/N ratios shown in Fig. 6. The average mobilities and carrier concentrations determined by Hall measurements on 0.5-mm- and 1–μm-thick GaN films grown under the conditions indicated in Fig. 6 by the closed circles and the open circle, respectively, are given in Table 1. The mobilities of the GaN films appear to change with Ga flux and, hence, growth regime. Samples grown under N-stable conditions were highly resistive. All of the Ga-stable samples were conductive and had relatively high mobilities. Within the intermediate regime, the mobility increased with Ga flux from 850 to 1100 cm^2/V·s. However, the mobility dropped substantially for the films grown within the Ga-droplet regime. The mobility appears to peak at the highest Ga flux achievable in the intermediate regime just below the boundary line. The average and the highest mobilities in samples grown under the last condition were 1100 and 1190 cm^2/V·s, respectively. These are among the highest RT mobilities reported for GaN and indicate that the MBE growth conditions have been optimized. The last two values are higher than previously reported and may be due to a reduction in the point defects or complexes for this sample [42]. The substantial decrease in mobility values, shown in Table 1, for the sample grown in the Ga droplet regime is due to the deleterious effects of these droplets. The morphological, optical, and electrical properties of the GaN under the Ga droplets are also inferior to the surrounding material [43].

As noted above, the commonly introduced acceptor is Mg, which has a thermal activation energy of ~120–200 MeV. Very sharp Mg doping profiles, both at the upper and lower interfaces for buried finite-thickness radio-frequency (RF) plasma MBE-grown layers, and hole mobilities and carrier concentrations comparable to the state-of-the-art MOVPE material have been reported [44] without the necessity for thermal annealing or the presence of the aforementioned "Mg memory" effect that is common in MOVPE reactors. The highest hole mobilities and the best surface morphologies for MBE-derived GaN have been observed at the crossover from the intermediate Ga-rich regime to the Ga-droplet regime in the growth diagram [45].

RF-plasma MBE has also been very successfully used for the development of high mobility 2-D electron gases (2DEGs) in the AlGaN/GaN system. For growth on Ga polar templates, a fixed positive sheet charge exists at the AlGaN/GaN interface due to the discontinuity in the total polarization between AlGaN and GaN. When the AlGaN cap layer exceeds a minimum thickness, a 2DEG forms at the interface. Contrary to results in MOVPE AlGaN/GaN structures, the 2DEG mobility for MBE AlGaN/GaN structures decreases with increasing sheet carrier concentration [46]. This indicates that the dominant scattering mechanism in MBE structures is either alloy scattering or interface roughness and not ionized impurity scattering. Thus, the highest mobilities in MBE structures have been realized at low Al concentrations and now exceed 60 000 $cm^2/V{\cdot}s$ at 4 K [47], a value about twice as large as reported in the best MOVPE AlGaN/GaN structures. This overall improvement in mobility is likely due to the reduction in unintentional impurity incorporation in the MBE environment. Similar to the results for n-GaN and p-GaN, 2DEGs with superior electrical properties are realized when the growth is conducted at the cross over from the intermediate Ga-rich regime to the Ga-droplet regime [48].

Thin films produced by any technique must be accompanied by characterization to provide both basic scientific understanding of the materials and to inform the grower regarding changes that must be made in the process route to achieve improved properties. Microstructural and electrical properties of the MOVPE and MBE films were described in the foregoing sections. However, these must be accompanied by optical and magnetic resonance studies to obtain important information regarding the vibrational characteristics; the presence, identity, and properties of intentionally and unintentionally introduced impurities that may or may not be electrically active; and the chemical identity and density of point defects and their magnetic properties. The following two sections address the capabilities and recent achievements in optical and magnetic resonance characterization of GaN films.

III. Optical Studies of Undoped and Doped GaN Semiconductors

A. Overview of Selected Techniques

PL is a sensitive and nondestructive technique for the detection and identification of impurities and other defects in semiconductors. Electrons and holes optically excited across the forbidden energy gap usually become localized or bound at an impurity or defect before recombining. The identity of the localized center to which they are bound can often be determined on the basis of the binding energies inferred from the spectral positions or from thermal quenching studies. Qualitative information regarding the structural and microstructural characteristics can be accessed from the efficiency and line widths of near band edge PL spectra. A broad scope of phenomena such as excitation, recombination mechanisms, structural defects, and impurities can be investigated. In general, a number of defects present simultaneously in the material can compete at different rates for the photo-excited carriers resulting in radiative or nonradiative recombination processes. Therefore, PL is not adequate to provide the concentration of defects.

Raman scattering (RS) allows one to study vibrational phenomena in solids. Inelastic light scattering in crystals is susceptible to selection rules originating from momentum conservation [49]. Therefore, RS can be used to assess both the structure and microstructure of bulk and epitaxial layers.

Fourier transform infrared (FTIR) absorption is a nondestructive technique to quantify neutral electrically active donors and acceptors. Photons with energies equal to the energy necessary to promote electrons or holes from the ground state to the excited states can be absorbed yielding an intrinsic optical signature of the donors and acceptors. Providing that the excited states are bound to the band by an energy that depends weakly on the nature of the donor or acceptor, the ground-to-excited state transitions of different donors/acceptors are relatively displaced by approximately the difference between their ground state binding energies.

B. Recent Progress in the Optical Characterization of GaN Thin Films

In 1971, Dingle *et al.* reported a seminal paper on low-temperature PL and reflectance studies of GaN films [50]. Films with thicknesses between 5–20 μm (type II) and between 100–250 μm (type I) had carrier concentrations of $\sim 10^{18}$ cm^{-3} and $\sim 10^{17}$ cm^{-3}, respectively. Intense and sharp PL lines and sharp reflectance lines, both assigned to free- and donor-bound excitons, were hallmarks of the improvements in the crystal structure and the microstructure of the films. However, the nature of the background donor (donors) was not known. Acceptor-type doping was very difficult as a result of the high-background n-type carrier concentration. The continuous progress in various growth techniques in combination with the use of an intermediary ("buffer") nucleation layer (NL) has resulted in a considerable reduction in the concentration of background donors [51], [52]. Unintentionally doped (UID) GaN films with high breakdown voltages (10^{10} Ω-cm) and n-type ($\leq 3 \times 10^{17}$ cm^{-3}) layers with high mobilities (~600 $cm^2/V{\cdot}s$) have been grown [53]. A typical PL spectrum of high resistivity films grown by MOVPE shows the so-called yellow band (2.25 eV) and a blue band around 3.0 eV, which may involve defects responsible for the partial compensation of these films. The sharp lines observed near 3.478 eV have been assigned to recombination

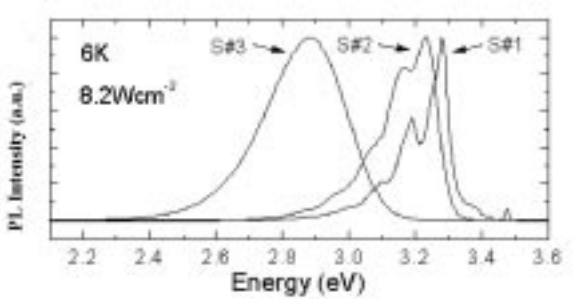

Fig. 7. Normalized low-temperature PL spectra of three GaN : Mg HE films deposited by MOCVD on a-face sapphire. Note the line shape change and the red-shift of the peak position with increasing Mg concentration, from 2.5×10^{18} to 7×10^{19} cm^{-3}. These samples have been postgrowth thermal annealed at 950 °C. Spectra are corrected for instrumental response.

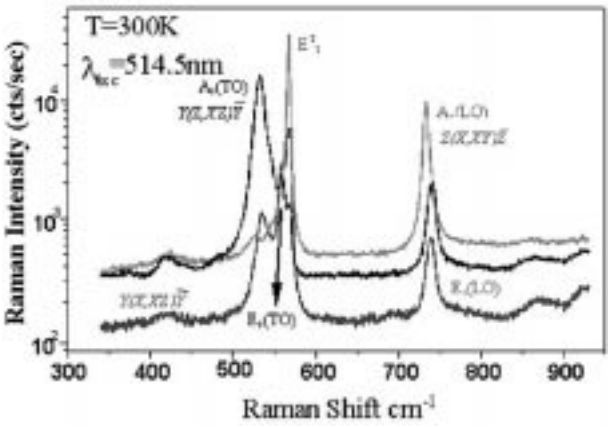

Fig. 8. First-order polarized RS spectra of a ~170-μm-thick freestanding GaN template. These spectra are consistent with high crystalline quality relaxed material.

processes associated with the annihilation of free-excitons (FEs) and excitons bound to a neutral shallow donor (D^{o}X) [54], [55]. Typical values of the D^{o}X full-width-at-half-maximum (FWHM) linewidth at 6 K are $\leq$3 MeV and for FE at 300 K $\leq$ 33 MeV for good UID heteroepitaxial (HE) layers [54]. The RS spectra of such materials showed all the six allowed modes with small FWHM values, which are consistent with wurtzite films without high values of residual stress. The PL spectrum of a typical Si-doped film consists of a weak 2.25-eV band and an intense edge emission assigned to a recombination process associated with X–Si^o (i.e., excitons bound to shallow Si donors). Films deposited with these optimized growth conditions have been successfully used for fabrication of high-yield field-effect transistors [56].

As noted above, Mg has a binding energy of $\geq$200 MeV in GaN. As such, only about 1% of the atoms are electrically active at RT. Therefore, a higher doping level is required to provide the RT hole concentrations necessary for device fabrication. However, a deep compensating donor is apparently introduced with increasing activated Mg concentration. The 6-K PL spectra of three GaN films doped with different concentrations of Mg are shown in Fig. 7. Note the shift between curves (a) and (b) and between (b) and (c). The first shift originates from potential fluctuations induced by charged donor and acceptor centers and the latter is assigned to a recombination process involving a deep donor and the Mg acceptor [57], [58].

C. Optical Properties of the State-of-the-Art GaN Films

The structural and optical properties of homoepitaxial GaN films can be used as a benchmark to which HE GaN films may be compared [59]. To reduce the usual high density of structural defects in HE layers, patterned HE GaN films have been developed for selective deposition of low defect density GaN overlayers, as described in Section I. TEM and X-ray diffraction studies of these LEO layers show that the LEO region contains a lower density of dislocations [60]. However, the regions of coalescence of the lateral growth fronts are characterized by a high concentration of extended defects resulting from the tilting and resultant crystallographic misalignment described in Section I. This problem is considerably reduced in the PE films also described in Section I. Another approach to control the propagation of dislocations in HE layers has been the growth of multiple GaN layers with intermediary AlN low-temperature NLs. A considerable increase in carrier mobility has been reported using this approach that may be associated with the reduction in the density of the threading screw dislocations; however, incorporation of a large concentration of donors has been observed in these UID highly strained layers [61].

Freestanding films (FSs) of GaN grown via hydride vapor phase epitaxy (HVPE) with a thickness of ~400 μm have been removed from sapphire substrates by laser-assisted liftoff, mechanically polished and reactive-ion etched to yield ~200-μm-thick flat and smooth templates that can be used for homoepitaxial growth [62]. These substrates possess a low background donor concentration ($\leq 2 \times 10^{16}$ cm^{-3}) and a very high mobility ($\geq$1200 cm^2/V·s) at RT [62]. Raman spectra of such films are consistent with X-ray diffraction studies and indicate that the crystallography and defect microstructure of these substrates surpass those of the best conventional MOVPE films and, in contrast to the latter films, possess a low residual strain [63]. The first-order Raman spectra of a representative FS GaN sample measured at RT for different sample orientations and light polarizations are shown in Fig. 8. High-resolution low-temperature PL spectra of a 12-μm-thick HE (dotted line, sample 1) film and of a 150-μm-thick (sample 2) FS HVPE GaN film are shown in Fig. 9. The spectrum of the FS template shows, in the 3.46–3.52-eV region, emission lines assigned to the ground and excited states of the FE A (labeled FX^1_A and FX^2_A, respectively) and the dominant D^{o}X [54], [55]. At ~3.45 eV, the two-electron satellite spectrum resulting from the recombination processes in which the D^o is left in an excited state after the excitons annihilation is observed. Also observed are the one-phonon replicas of all features listed above for energies below 3.42 eV. The spectrum of sample 1 shows most of the observed features. However, all features are smeared and shifted to higher energy due to inhomogeneous broadening and the residual compressive strain. The FWHM of the D^{o}X for sample 1 is

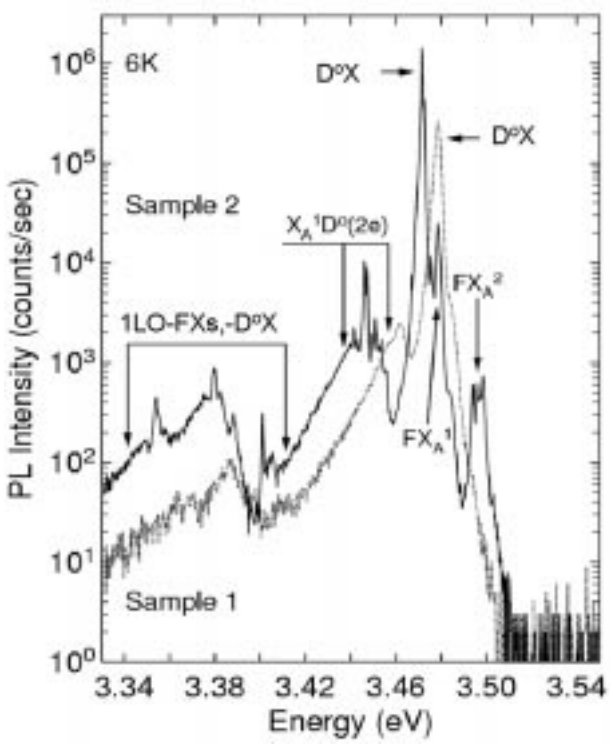

Fig. 9. High-resolution band edge PL spectra of two representative HVPE samples. Sample 1 is still on the sapphire substrate and sample 2 was removed using a laser liftoff technique. Presence of a variety of sharp excitonic lines in this spectral region confirms the single crystalline nature and the low densities of dislocations and other defects in both samples.

2.69 MeV; for sample 2, it is only 370 μeV [64]. A 6.2-MeV shift to higher energy resulting from the compressive strain has been measured for sample 1. The results of detailed FTIR and secondary ion mass spectrometry (SIMS) studies conducted on these samples have revealed two pervasive donors. The more shallow and the deeper donors are Si and O, with binding energies of 30.19 $\pm$ 0.1 MeV and 33.21 $\pm$ 0.1 MeV, respectively [65].

IV. Characterization of Defects in GaN and Related Alloys by Magnetic Resonance Techniques

A. Overview of the Techniques

The interaction of the electronic spin and an applied magnetic field splits the ground and excited states associated with point defects, e.g., dopants, transition metals, vacancies, interstitial atoms, and antisites, into two or more levels. In principle, transitions between these levels can be detected by spin resonance techniques such as electron paramagnetic resonance (EPR) and optically detected magnetic resonance (ODMR). In addition to giving important information such as chemical identification of the defect through Zeeman splittings (g factors) and resolved hyperfine (HF) structure, EPR can provide a quantitative measure of the defect densities in the material. Though not quantitative, ODMR combines the attributes of EPR with the sensitivity and selectivity of PL. In particular, this technique gives information on the magnetic properties of the optically excited donor and acceptor states, e.g., that participate directly (or sometimes indirectly) in radiative recombination processes [66].

B. Magnetic Resonance Research on III-Nitrides

Very little magnetic resonance work on GaN and related materials was reported prior to 1990. One example is the nuclear magnetic resonance (NMR) experiments performed on GaN bulk powders that gave the magnitude of the electric field gradients at the host lattice sites [67]. In parallel with the dramatic advances in materials growth and device development, an international effort has been ongoing since that time to obtain a better understanding of the properties of residual defects and dopants in GaN through magnetic resonance techniques. Most of the EPR and ODMR have been performed on as-grown (n-type and highly resistive) and Si-, Mg-, or Be-doped wurtzite (hexagonal) GaN HE layers [68]–[72] with little work reported for zincblende (cubic) GaN [73]. Some research (mainly EPR) has been conducted on n-type (as-grown or Si-doped) $Al_xGa_{1-x}N$ HE layers [74], [75] and, surprisingly, little magnetic resonance has been reported for InGaN epitaxial layers with the exception of $In_xGa_{1-x}N$-based light-emitting diode structures [76], [77].

A variety of defects of donor and acceptor character have been revealed by EPR, ODMR, and related techniques in these GaN-based materials and device structures. However, their microscopic identities have been a challenge based on the absence of resolved HF structure in most cases. Some exceptions where defect identification has been possible include residual transition metals in GaN such as Fe, Ni, Mn, and Cu as well as Ga interstitial-related defects observed recently by ODMR on IR emission from electron-irradiated GaN [78]. Examples of magnetic resonance characterization of defects in GaN and related alloys are given below.

The EPR spectra obtained at 9.5 GHz for as-grown (n-type) GaN and $Al_xGa_{1-x}N$ ($x = 0.12$ and 0.26) HE layers grown on 6H–SiC(0001) by MOVPE are shown in the top half of Fig. 10. A single line with axial symmetry about the c axis with $g_{||} = 1.9515$ and $g_{\perp} = 1.9485$ is found from the GaN film and has been firmly established as a "fingerprint" for shallow donors/conduction electrons [68]. The small shift (i.e., $\Delta g \sim 0.05$) from the free-electron g value of 2.0023 is in good agreement with that predicted from multiband k·p effective-mass (EM) theory [68], [75]. It is generally agreed that likely candidates for residual shallow donors in these materials are Si and O. Unfortunately, in contrast to the case of Si, where the EPR is much sharper and different donors could be distinguished by their g values [79], it is not expected that a difference in g values can be detected for shallow donors with similar binding energies in GaN. For the EPR of shallow donors in $Al_xGa_{1-x}N$, the monotonic increase of the g values (see inset in Fig. 10) toward the value of two with increasing Al mole fraction reflects the decrease in spin-orbit splittings of the valence and upper conduction bands and the increase of the interband energies [74], [75].

EPR is particularly useful to determine the neutral acceptor concentrations in p-type Mg-doped GaN without

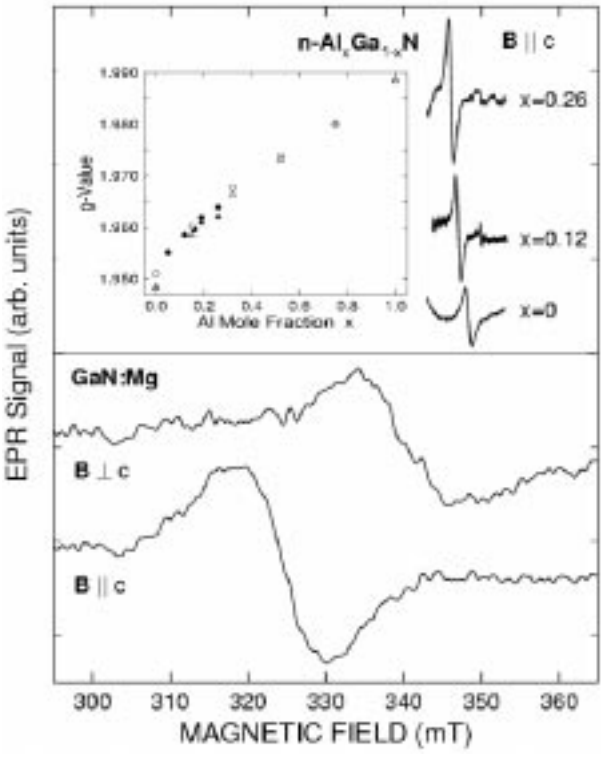

Fig. 10. Top: EPR spectra found at 9.5 GHz for as-grown (n-type) GaN and $Al_xGa_{1-x}N$ epitaxial layers. Also shown is a plot of the donor g values versus Al mole fraction. Closed symbols are from [74], open symbols are from [75]. Circles: g factors with **B** $\|$ c; triangles: g factors with **B** $\perp$ c. Bottom: EPR spectra for a Mg-doped (p-type) GaN film.

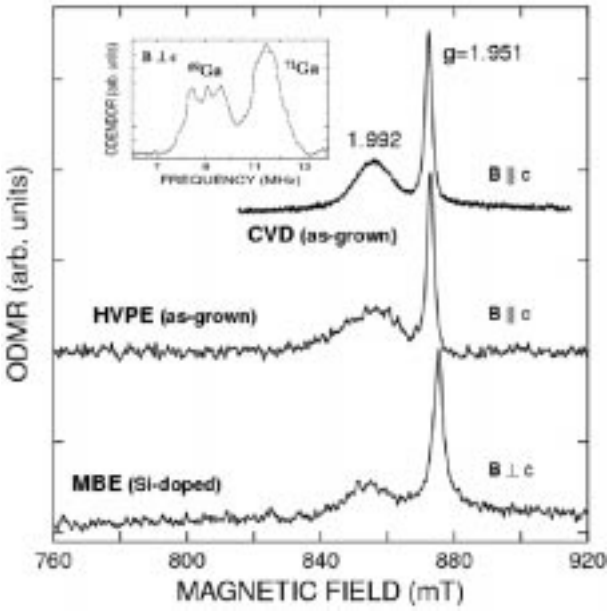

Fig. 11. ODMR obtained at 24 GHz on the 2.2-eV "yellow" PL band from n-type GaN grown by CVD, HVPE, and MBE. Inset: ODENDOR spectra found on the shallow donor resonance from an as-grown (highly resistive) GaN sample [83]. Features are attributed to ^{69,71}Ga host lattice nuclei that sense the WZ crystal field and local strains through the nuclear quadrupole interaction. Similar ODENDOR has been reported on the $g = 1.992$ deep defect ODMR [71].

the need for contacts or the high temperatures required (due to the large ionization energy of ∼200 MeV) for Hall effect measurements. For example, representative spectra obtained for a Mg-doped GaN sample grown on sapphire by MOVPE with a RT free hole carrier density of $\sim 1.7 \times 10^{17}$ cm^{-3} are shown in the bottom half of Fig. 10. A single resonance is found with $g_{||} = 2.10$ and $g_{\perp} = 1.99$ and a spin density of $\sim 4 \times 10^{19}$ cm^{-3}. This feature is assigned to shallow Mg acceptors based on the similarity of the EPR spin density with the concentration of electronically active Mg acceptors determined by temperature-dependent Hall effect and the total Mg level as revealed by SIMS. In addition, similar magnetic resonance parameters have been found from ODMR studies of shallow Mg acceptors [80] involved in shallow donor–shallow acceptor recombination (ZPL at ∼3.27 eV) from Mg-doped GaN.

The PL most studied in GaN by ODMR during the last decade is the ubiquitous 2.2-eV emission band [69]–[71]. The spectra obtained using this technique at 24 GHz from n-type (as-grown or Si-doped) GaN epitaxial layers grown by MOVPE, HVPE, and MBE are shown in Fig. 11. The spectra are very similar in spite of the radically different growth techniques. The sharp line with $g_{||} = 1.951$ and $g_{\perp} = 1.948$ is assigned to (EM) shallow donors based on the EPR work [68]. Most groups associate the broader feature with $g_{||} = 1.989$ and $g_{\perp} = 1.992$ to deep defects. This center was first assigned to deep donors [69] from the small negative g-shift relative to the free-electron g-value of 2.0023. However, based on the observation of similar g-shifts for Mg-shallow acceptors in subsequent EPR and ODMR studies (e.g., $g_{\perp} = 1.99$), the donor or acceptor character of this deep center is an open question from a magnetic resonance viewpoint. It has been suggested from the results of other techniques [81] and theory [82] that deep levels, associated with Ga vacancies or their complexes, are involved in 2.2-eV PL. More sophisticated magnetic resonance techniques have been applied to determine the origins of both this deep defect and residual shallow donors in GaN. In particular, several groups have performed optically detected electron-nuclear double-resonance experiments [71], [83], [84] on the 2.2-eV band, but evidence has only been found for NMR associated with ^{69,71}Ga lattice nuclei (see inset in Fig. 11).

Researchers at Lehigh University have recently demonstrated an elegant example of the potential of magnetic resonance to provide microscopic identification of defects in GaN [78]. In particular, isolated interstitial Ga atoms were observed in undoped (n-type) GaN after irradiation *in-situ* at 4.2 K with 2.5-MeV electrons. In addition to the EM donor signal, a new defect (referred to as L5) was observed with well-resolved HF structure due to a single I = 3/2 Ga nucleus. The spectra are composed of two sets of four lines associated with the two Ga nuclear isotopes (^{69}Ga, 60% abundant; ^{71}Ga, 40% abundant). The strength of the HF interaction ($A_{||,\perp} \sim 4$ GHz) that describes the coupling between the electronic and nuclear spins indicates that L5 is a deep level. Overall, these results provide great promise for identification of other lattice defects in GaN and related materials.

V. Summary

HE growth of (Al, In, Ga)N compounds and alloys at high rates, excellent compositional control, and uniformity over large areas, low background carrier concentrations, and donor (Si) and acceptor (Mg) doping have been accomplished via MOVPE on sapphire, SiC, and bulk GaN substrates. However, the Mg memory effect in the system is a significant problem. LEO and/or PE produce GaN and AlGaN continuous layers with a reduced density of dislocations, a reduced strain, and strong sharp optical emission; however, tilting and coalescence boundaries are produced by the laterally growing material.

Very high electron mobilities in both n-type GaN and in 2DEGs at the AlGaN/GaN interface have been realized by RF plasma-assisted MBE of these materials on thin-film GaN substrates at the crossover from the intermediate growth regime to the droplet regime in the growth diagram. Transport properties and the sharpness of the Mg doping profiles in p-type GaN exceed the best achieved via MOVPE. In addition, there is no Mg memory effect. Heterogeneous growth, substrate temperature uniformity, and flux control are the significant challenges for MBE.

PL results of MOVPE-derived UID HE GaN films showed sharp lines near 3.478 eV due to recombination processes associated with the annihilation of FEs and excitons bound to a neutral shallow donor (D^oX). For good HE films, FWHM linewidths for D^oX at 6 K are $\leq$3 MeV and for FE at 300 K are $\leq$33 MeV. The RS spectra of such materials showed all the six allowed modes with small FWHM values. The PL spectrum of a typical Si-doped film consists of a weak 2.25-eV band and an intense edge emission assigned to recombination process associated with X–Si^o. A deep compensating donor is introduced with increasing concentration of the Mg acceptor. The spectrum of HVPE-derived FS GaN templates shows, within the 3.46–3.52-eV region, emission lines assigned to the excited state of the FE A (FX_A^1) and the dominant D^oX. At $\sim$ 3.45 eV, the two-electron satellite spectrum resulting from the recombination processes in which the D^o is left in an excited state after the excitons annihilation is observed. FTIR and SIMS studies conducted on the FS samples have revealed the pervasive donors to be Si and O.

The EPR for n-type GaN and $Al_xGa_{1-x}N$ HE layers shows single lines with axial symmetry about the c axis with $g_{||}$ and $g_{\perp}$ between 1.94 and 1.99. This has been established as a "fingerprint" for shallow donors/conduction electrons. EPR for p-type GaN samples reveals a single resonance feature with $g_{||} = 2.10$ and $g_{\perp} = 1.99$, which has been assigned to shallow Mg acceptors. ODMR of the 2.2-eV emission band from n-type GaN epitaxial layers grown by MOVPE, HVPE, and MBE are similar. The sharp line with $g_{||} = 1.951$ and $g_{\perp} = 1.948$ has been assigned to shallow donors. Most groups associate the broader feature with $g_{||} = 1.989$ and $g_{\perp} = 1.992$ to deep defects whose electronic character remains controversial. ODMR measurements of electron-irradiated GaN have identified the Ga_i based on well-resolved HF structure.

References

[1] S. Jingxi, J. M. Redwing, and T. F. Kuech, "Model development of GaN MOVPE growth chemistry for reactor design," *J. Electron. Mater.*, vol. 29, pp. 2–9, Jan. 2000.

[2] N. Elmasry, E. Piner, S. Liu, and S. Bedair, "Phase separation in InGaN grown by metal–organic chemical vapor deposition," *Appl. Phys. Lett.*, vol. 72, pp. 40–42, Jan. 1998.

[3] M. McCluskey, L. Romano, B. Krusor, D. Bour, N. Johnson, and N. Brennan, "Phase separation in InGaN/GaN multiple quantum wells," *Appl. Phys. Lett.*, vol. 72, pp. 1730–1732, Apr. 1998.

[4] S. M. Bedair, F. G. McIntosh, J. C. Roberts, E. L. Piner, K. S. Boutros, and N. A. El-Masry, "Growth and characterization of in-based nitride compounds," *J. Cryst. Growth*, vol. 178, pp. 32–44, June 1997.

[5] S. Keller, B. P. Keller, D. Kapolnek, U. K. Mishra, S. P. DenBaars, I. K. Shmagin, R. M. Kolbas, and S. Krishnankutty, "Growth of bulk InGaN films and quantum wells by atmospheric pressure metal–organic chemical vapor deposition," *J. Cryst. Growth*, vol. 170, pp. 349–352, Jan. 1997.

[6] S. Keller, B. P. Keller, D. Kapolneck, A. C. Abare, H. Masui, L. A. Coldren, U. K. Mishra, and S. P. DenBaars, "Growth and characterization of bulk InGaN films and quantum wells," *Appl. Phys. Lett.*, vol. 68, pp. 3147–3149, May 1996.

[7] S. Nakamura, "GaN growth using GaN buffer layer," *Jpn. J. Appl. Phys.*, vol. 30, pp. L1705–L1707, Oct. 1991.

[8] H. Amano, N. Sawaki, I. Akasaki, and Y. Toyoda, "Metal–organic vapor phase epitaxial growth of a high quality GaN film using an AlN buffer layer," *Appl. Phys. Lett.*, vol. 48, pp. 353–355, Feb. 1986.

[9] W. Weeks, M. D. Bremser, K. Ailey, E. Carlson, W. Perry, and R. F. Davis, "GaN thin films deposited via organometallic vapor phase epitaxy on 6H–SiC(0001) using high-temperature monocrystalline AlN buffer layers," *Appl. Phys. Lett.*, vol. 67, pp. 401–403, May 1995.

[10] C. Van de Walle, C. Stampfl, and J. Neugebauer, "Theory of doping and defects in III–V nitrides," *J. Cryst. Growth*, vol. 189/190, pp. 505–510, June 1998.

[11] A. J. Ptak, L. J. Holbert, C. H. Swartz, L. Wang, N. C. Giles, T. H. Myers, G. C. B. Braga, J. A. Freitas, D. D. Koleske, R. L. Henry, A. E. Wickenden, C. Tian, A. Hockett, S. Mithra, and P. Van Lierde, presented at the 43rd Electronic Materials Conf., Notre Dame, IN, 2001.

[12] H. Amano, M. Kito, K. Hiramatsu, and I. Akasaki, "P-type conduction in Mg-doped GaN treated with low-energy electron beam irradiation (LEEBI)," *Jpn. J. Appl. Phys.*, pt. 2, vol. 28, pp. L2112–L2114, Dec. 1989.

[13] S. Nakamura, "Thermal annealing effects on P-type Mg-doped GaN films," *Jpn. J. Appl. Phys.*, vol. 31, pp. L139–L142, Feb. 1992.

[14] W. Gotz, N. M. Johnson, J. Walker, D. P. Bour, and R. A. Street, "Activation of acceptors in Mg-doped GaN grown by netalorganic chemical vapor deposition," *Appl. Phys. Lett.*, vol. 68, pp. 667–669, Jan. 1996.

[15] M. Miyachi, T. Tanaka, Y. Kiumur, and H. Ota, "The activation of Mg in GaN by annealing with minority-carrier injection," *Appl. Phys. Lett.*, vol. 72, pp. 1101–1103, Mar. 1998.

[16] M. D. Bremser, W. G. Perry, O. H. Nam, D. P. Griffis, R. Loesing, D. A. Ricks, and R. F. Davis, "Acceptor and donor doping of AlGaN thin film alloys grown on 6H–SiC(0001) substrates via metal–organic vapor phase epitaxy," *J. Electron. Mater.*, vol. 27, pp. 229–232, Apr. 1998.

[17] T. Sugahara, H. Sato, M. Hao, Y. Naoi, S. Kurai, S. Tottori, K. Yamashita, K. Nishino, L. T. Romano, and S. Sakai, "Direct evidence that dislocations are nonradiative recombination centers in GaN," *Jpn. J. Appl. Phys.*, vol. 37, pp. L398–L400, Apr. 1998.

[18] M. Leszczynski, B. Beaumont, E. Frayssinet, W. Knap, P. Prystawko, T. Suski, I. Grzegory, and S. Porowski, "GaN homoepitaxial layers grown by metal–organic chemical vapor deposition," *Appl. Phys. Lett.*, vol. 75, pp. 1276–1278, Aug. 1999.

[19] C. Kirchner, V. Schwegler, F. Eberhard, M. Kamp, K. J. Ebeling, K. Kornitzer, T. Ebner, K. Thonke, R. Sauer, P. Prystawko, M. Leszczynski, I. Grzegory, and S. Porowski, "Homoepitaxial growth of GaN by metal–organic vapor phase epitaxy: A benchmark for GaN technology," *Appl. Phys. Lett.*, vol. 75, pp. 1098–1100, Aug. 1999.

[20] B. Beaumont, M. Vaille, G. Nataf, A. Bouille, J. C. Guillaume, P. Vennegues, S. Haffouz, and P. Gibart, "Mg-enhanced lateral overgrowth of GaN on patterned GaN/sapphire substrate by selective metal organic vapor phase epitaxy," *MRS Internet J. Nitride Semicond. Res.*, vol. 3, p. 20, 1998.

[21] O. H. Nam, M. D. Bremser, T. S. Zheleva, and R. F. Davis, "Lateral epitaxy of low defect density GaN layers via organometallic vapor phase epitaxy," *Appl. Phys. Lett.*, vol. 71, pp. 2638–2640, Nov. 1997.

[22] S. Nakamura, "InGaN/GaN/AlGaN-based laser diodes with an estimated lifetime of longer than 10 000 hours," *MRS Bullet.*, vol. 23, pp. 37–43, May 1998.
[23] O. H. Nam, T. S. Zheleva, M. D. Bremser, and R. F. Davis, "Lateral epitaxial overgrowth of GaN films on SiO_2 areas via metal–organic vapor phase epitaxy," *J. Electron. Mater.*, vol. 27, pp. 233–237, Mar. 1998.
[24] T. Zheleva, S. Smith, D. Thomson, and K. Linthicum, "Pendeo-epitaxy—A new approach for lateral growth of gallium nitride films," *J. Electron. Mater.*, vol. 28, pp. L5–L8, Apr. 1999.
[25] R. F. Davis, T. Gehrke, K. J. Linthicum, T. S. Zheleva, E. A. Preble, P. Rajagopal, C. A. Zorman, and M. Mehregany, "Pendeo-epitaxial growth of thin films of gallium nitride and related materials and their characterization," *J. Cryst. Growth*, vol. 225, pp. 134–140, May 2001.
[26] T. Gehrke, K. J. Linthicum, E. Preble, P. Rajagopal, C. Ronning, C. Zorman, M. Mehregany, and R. F. Davis, "Pendeo-epitaxial growth of gallium nitride on silicon substrates," *J. Electron. Mater.*, vol. 29, pp. 306–310, Mar. 2000.
[27] F. Bertram, T. Riemann, J. Christen, A. Kaschner, A. Hoffmann, C. Thomsen, K. Hiramatsu, T. Shibata, and N. Sawaki, "Strain relaxation and strong impurity incorporation in epitaxial laterally overgrown GaN: Direct imaging of different growth domains by cathodoluminescence microscopy and micro-raman spectroscopy," *Appl. Phys. Lett.*, vol. 74, pp. 359–361, Jan. 1999.
[28] T. Gehrke, K. J. Linthicum, D. B. Thomson, P. Rajagopal, A. D. Batchelor, and R. F. Davis, "Pendeo-epitaxy of gallium nitride and aluminum nitride films and heterostructures on silicon carbide substrate," *MRS Internet J. Semicond. Res.*, vol. 4S1, 1999.
[29] H. Heinke, V. Kirchner, S. Einfeldt, and D. Hommel, "Analysis of the defect structure of epitaxial GaN," *Phys. Stat. Sol. (a)*, vol. 176, pp. 391–395, Nov. 1999.
[30] C. Kisielowski, J. Kruger, S. Runimov, T. Suski, J. W. Ager, III., E. Jones, Z. Liliental-Weber, M. Ruben, E. R. Weber, M. D. Bremser, and R. F. Davis, "Strain-related phenomena in GaN thin films," *Phys. Rev. B*, vol. 54, pp. 17 745–17 753, Dec. 1996.
[31] A. M. Roskowski, P. Q. Miraglia, E. A. Preble, S. Einfeldt, T. Stiles, R. F. Davis, J. Schuck, R. Grober, and U. Schwarz, "Strain and dislocation reduction in maskless pendeo-epitaxy GaN thin films," *Phys. Stat. Sol. (a)*, vol. 188, no. 2, pp. 729–732, Nov. 2001.
[32] E. J. Tarsa, B. Heying, X. H. Wu, P. Fini, S. P. DenBaars, and J. S. Speck, "Homoepitaxial growth of GaN under Ga-stable and N-stable conditions by plasma-assisted molecular beam epitaxy," *J. Appl. Phys.*, vol. 82, no. 11, pp. 5472–5479, Dec. 1997.
[33] X. H. Wu, L. M. Brown, D. Kapolnek, S. Keller, B. Keller, S. P. DenBaars, and J. S. Speck, "Defect structure of metal-organic chemical vapor deposition-grown epitaxial (0001) GaN/Al_2O_3," *J. Appl. Phys.*, vol. 80, no. 6, pp. 3228–3237, Sept. 1996.
[34] S. M. Newstead, R. A. A. Kubiak, and E.H.C. Parker, "On the practical applications of MBE surface phase diagrams," *J. Cryst. Growth*, vol. 81, no. 1–4, pp. 49–54, Feb. 1987.
[35] S. Y. Karpov, Y. V. Kovalchuk, V. E. Myachin, and Y. V. Pogorelskii, "Instability of III–V compound surfaces due to liquid phase formation," *J. Cryst. Growth*, vol. 129, no. 3–4, pp. 563–570, Apr. 1993.
[36] H. Okumura, K. Balakrishnan, H. Hamaguchi, T. Koizumi, S. Chichibu, H. Nakanishi, T. Nagatomo, and S. Yoshida, "Analysis of MBE growth mode for GaN epilayers by RHEED," *J. Cryst. Growth*, vol. 189/190, pp. 364–369, June 1998.
[37] R. Held, D. E. Crawford, A. M. Johnston, A. M. Dabiran, and P. I. Cohen, "*In situ* control of GaN growth by molecular beam epitaxy," *J. Electron. Mater.*, vol. 26, no. 3, pp. 272–280, Mar. 1997.
[38] R. Held, G. Nowak, B. E. Ishaug, S. M. Seutter, A. Parkhomovsky, A. M. Dabiran, P. I. Cohen, I. Grzegory, and S. Porowski, "Structure and composition of GaN(0001) A and B surfaces," *J. Appl. Phys.*, vol. 85, no. 11, pp. 7697–7704, June 1999.
[39] H. Riechert, R. Averbeck, A. Graber, M. Schienle, U. Strauss, and H. Tews, "Optimized structural properties of wurtzite GaN on SiC(0001) grown by molecular beam epitaxy," *Proc. Mater. Res. Soc. Symp.*, vol. 449, pp. 149–159, 1997.
[40] P. Hacke, G. Feuillet, H. Okumura, and S. Yoshida, "Monitoring surface stoichiometry with the (2×2) reconstruction during grwth of hexagonal phase GaN by molecular beam epitaxy," *Appl. Phys. Lett.*, vol. 69, no. 17, pp. 2507–2509, Oct. 1996.
[41] B. Heying, R. Averbeck, L. F. Chen, E. Haus, H. Riechert, and J. S. Speck, "Dislocation mediated surface morphology of GaN," *J. Appl. Phys.*, vol. 88, no. 4, pp. 1855–1860, Aug. 2000.
[42] B. Heying, I. Smorchkova, C. Poblenz, C. Elsass, P. Fini, S. Den Baars, U. Mishra, and J. S. Speck, "Optimization of the surface morphologies and electron mobilities in GaN grown by plasma-assisted molecular beam epitaxy," *Appl. Phys. Lett.*, vol. 77, no. 18, pp. 2885–2887, Oct. 2000.
[43] B. Heying, T. Myers, and J. S. Speck, unpublished data.
[44] I. P. Smorchkova, E. Haus, B. Heying, P. Kozodoy, P. Fini, J. P. Ibbetson, S. Keller, S. P. DenBaars, J. S. Speck, and U. K. Mishra, "Mg doping of GaN layers grown by plasma-assisted molecular-beam epitaxy," *Appl. Phys. Lett.*, vol. 76, no. 6, pp. 718–720, Feb. 2000.
[45] E. Haus, Y. Smorchkova, B. Heying, U. K. Mishra, S. P. DenBaars, and J. S. Speck, unpublished data.
[46] I. P. Smorchkova, C. R. Elsass, J. P. Ibbetson, R. Vetury, B. Heying, P. Fini, E. Haus, S. P. DenBaars, J. S. Speck, and U. K. Mishra, "Polarization-induced charge and electron mobility in AlGaN/GaN heterostructures grown by plasma-assisted molecular-beam epitaxy," *J. Appl. Phys.*, vol. 86, no. 8, pp. 4520–4526, Oct. 1999.
[47] C. R. Elsass, I. P. Smorchkova, B. Heying, E. Haus, C. Poblenz, P. Fini, K. Maranowski, P. M. Petroff, S. P. DenBaars, U. K. Mishra, J. S. Speck, A. Saxler, S. Elhamri, and W. C. Mitchel, "Effects of growth conditions on the incorporation of oxygen in AlGaN layers grown by plasma assisted molecular beam epitaxy," *Jpn. J. Appl. Phys.*, vol. 39, no. 10B, pp. L1023–L1025, Oct. 2000.
[48] C. R. Elsass, C. Poblenz, B. Heying, P. Fini, P. M. Petroff, S. P. DenBaars, U. K. Mishra, and J. S. Speck, "Influence of Ga flux on the growth and electron transport properties of AlGaN/GaN heterostructures grown by plasma-assisted molecular beam epitaxy," *J. Cryst. Growth*, vol. 233, no. 4, pp. 709–716, Dec. 2001.
[49] M. Cardona, "Light scattering in solids," in *Topics in Applied Physics* Springer-Verlag, Germany, 1983, vol. 8.
[50] R. Dingle, D. D. Sell, S. E. Stokowski, and M. Ilegems, "Absorption, reflectance, and luminescence of GaN epitaxial layers," *Phys. Rev. B*, vol. 4, pp. 1211–1218, Aug. 1971.
[51] S. Yoshida, S. Misawa, and S. Gonda, "Improvements on the electrical and luminescence properties of reactive molecular beam epitaxially grown films by using AlN-coated sapphire substrates," *Appl. Phys. Lett.*, vol. 42, pp. 427–430, Mar. 1983.
[52] H. Amano, N. Sawaki, I. Akasaki, and T. Toyoda, "Metal–organic vapor phase epitaxial growth of a high quality GaN film using an AlN buffer layer," *Appl. Phys. Lett.*, vol. 48, pp. 353–355, Feb. 1986.
[53] A. E. Wickenden, L. B. Rowland, K. Doverspike, D. K. Gaskill, J. A. Freitas, Jr., D. S. Simons, and P. H. Chi, "Doping of galliun nitride using disilane," *J. Electron. Mater.*, vol. 24, pp. 1547–1550, Nov. 1995.
[54] J. A. Freitas, Jr., K. Doverspike, and A. E. Wickenden, "Excitonic recombination processes in doped and undoped wurtzite GaN films deposited on sapphire substrates," *Proc. Mater. Res. Soc. Symp.*, vol. 395, pp. 485–490, 1996.
[55] W. Shan, T. J. Schmidt, X. H. Yang, S. J. Huang, J. J. Song, and B. Goldenberg, "Temperature dependence of interband transitions in GaN grown by metal–organic chemical vapor deposition," *Appl. Phys. Lett.*, vol. 66, pp. 985–987, Feb. 1995.
[56] S. C. Binari, W. Kruppa, H. B. Dietrich, G. Kelner, A. E. Wickenden, and J. A. Freitas, Jr., "Fabrication and characterization of GaN FETs," *Solid-State Electron.*, vol. 41, pp. 1549–1554, Oct. 1997.
[57] M. A. Reshchikov, G.-C. Yi, and B. W. Wessels, "Behavior of 2.8- and 3.2-eV photoluminescence bands in Mg-doped GaN at different temperatures and excitation densities," *Phys. Rev. B*, vol. 59, pp. 13 176–13183, May 1999.
[58] H. Teisseyre, T. Suski, P. Perlin, I. Grzegory, M. Leszczynski, M. Bockowski, S. Porowski, J. A. Freitas, Jr., R. L. Henry, A. E. Wickenden, and D. D. Koleske, "Different character of the donor-acceptor pair-related 3.27-eV band and blue photoluminescence in Mg-doped GaN. Hydrostatic pressure studies," *Phys. Rev. B*, vol. 62, pp. 10 151–10 157, Oct. 2000.
[59] K. Kornitzer, T. Ebner, K. Thonke, R. Sauer, C. Kirchner, V. Schwegler, M. Kamp, M. Leszczynski, I. Grzegory, and S. Porowski, "Photoluminescence and reflectance spectroscopy of excitonic transitions in high-quality homoepitaxial GaN films," *Phys. Rev. B*, vol. 60, pp. 1471–1473, July 2000.
[60] J. A. Freitas, Jr., O.-K. Nam, R. F. Davis, G. V. Saparin, and S. K. Obyden, "Optical characterization of lateral epitaxial overgrown GaN layers," *Appl. Phys. Lett.*, vol. 72, pp. 2990–2293, June 1998.
[61] D. D. Koleske, M. E. Twigg, A.E. Wickenden, R. L. Henry, R. J. Gorman, J. A. Freitas, Jr., and M. Fatemi, "Properties of Si-doped GaN films grown using multiple AlN interlayers," *Appl. Phys. Lett.*, vol. 75, pp. 3141–3143, Nov. 1999.

[62] K. Lee and K. Auh, "Properties of freestanding GaN substrates grown by hydride vapor phase epitaxy," *Jpn. J. Appl. Phys.*, vol. 40, p. L13, Jan. 2001.
[63] J. A. Freitas, Jr., G. C. B. Braga, W. J. Moore, J. G. Tischler, J. C. Culbertson, M. Fatemi, S. S. Park, S. K. Lee, and Y. Park, "Structural and optical properties of thick freestanding GaN templates," *J. Cryst. Growth*, vol. 3, pp. 322–328, Oct. 2001.
[64] J. A. Freitas, Jr., G. C. B. Braga, W. J. Moore, S. K. Lee, K. Y. Lee, I. J. Song, R. J. Molnar, and P. Van Lierde, "Detection and identification of donors in hydride-vapor-phase-epitaxial GaN layers," *Phys. Solid State*, vol. 188, pp. 457–461, Nov. 2001.
[65] W. J. Moore, J. A. Freitas, Jr., G. C. B. Braga, R. J. Molnar, S. K. Lee, K. Y. Lee, and I. J. Song, "Identification of Si and O donors in Hydride-vapor-phase-epitaxial GaN," *Appl. Phys. Lett.*, vol. 79, pp. 2570–2572, Oct. 2001.
[66] T. A. Kennedy and E. R. Glaser, "Magnetic resonance of epitaxial layers detected by photoluminescencein," in *Identification of Defects in Semiconductors*, M. Stavola, Ed. New York: Academic, 1998, vol. 51A, Semiconductors and Semimetals, pp. 93–136.
[67] O. Han, H. K. C. Timken, and E. Oldfield, "Solid-state magic-angle sample-spinning nuclear magnetic resonance spectroscopic study of group III–V semiconductors," *J. Chem. Phys.*, vol. 89, pp. 6046–6052, Nov. 1988.
[68] W. E. Carlos, J. A. Freitas, Jr., M. Asif Khan, D. T. Olson, and J. N. Kuznia, "Electron-spin-resonance studies of donors in wurtzite GaN," *Phys. Rev. B*, vol. 48, pp. 17 878–17 884, Dec. 1993.
[69] E. R. Glaser, T. A. Kennedy, K. Doverspike, L. B. Rowland, D. K. Gaskill, J. A. Freitas, Jr., M. Asif Khan, D. T. Olson, J. N. Kuznia, and D. K. Wickenden, "Optically detected magnetic resonance of GaN films grown by organometallic chemical vapor deposition," *Phys. Rev. B*, vol. 51, pp. 13 326–13 336, May 1995.
[70] B. K. Meyer, "Magnetic resonance investigations of group-III nitrides," in *Semiconductors and Semimetals*, R. K. Willardson and E. R. Weber, Eds. New York: Academic, 1999, vol. 57, pp. 371–406.
[71] F. K. Koschnick, K. Michael, J.-M. Spaeth, B. Beaumont, P. Gibart, E. Calleja, and E. Munoz, "Optically detected magnetic resonance study of defects in undoped, Be-doped, and Mg-doped GaN," *J. Electron. Mater.*, vol. 29, pp. 1351–1355, Dec. 2000.
[72] E. R. Glaser *et al.*, "Characterization of nitrides by electron paramagnetic resonance (EPR) and optically detected magnetic resonance (ODMR)," *Mater. Sci. Eng. B*, vol. 93, no. 1–3, pp. 39–48, May 2002.
[73] M. Fanciulli, T. Lei, and T. D. Moustakas, "Conduction electron spin resonance in zinc-blende GaN thin films," *Phys. Rev. B*, vol. 48, pp. 15 144–15 147, Nov. 1993.
[74] W. E. Carlos, "Magnetic resonance studies of dopants and defects in GaN-based materials and devices," in *Proceedings of the 7th International Conference on Shallow Level Centers in Semiconductors*, C. A. J. Ammerlaan and B. Pajot, Eds. Singapore: World Scientific, 1997, p. 13.
[75] M. W. Bayerl, M. S. Brandt, T. Graf, O. Ambacher, J. A. Majewski, and M. Stutzmann, "g-values of effective mass donors in $Al_xGa_{1-x}N$ alloys," *Phys. Rev. B*, vol. 63, Apr. 2001.
[76] E. R. Glaser, T. A. Kennedy, W. E. Carlos, P. P. Ruden, and S Nakamura, "Recombination processes in $In_xGa_{1-x}N$ studied through optically detected magnetic resonance," *Appl. Phys. Lett.*, vol. 73, pp. 3123–3125, Nov. 1998.
[77] W. E. Carlos, E. R. Glaser, T. A. Kennedy, and S. Nakamura, "Magnetic resonance studies of InGaN- based quantum well diodes," *J. Electron. Mater.*, vol. 28, pp. 252–256, Mar. 1999.
[78] K. H. Chow, G. D. Watkins, A. Usui, and M. Mizuta, "Detection of interstitial Ga in GaN," *Phys. Rev. Lett.*, vol. 85, pp. 2761–2764, Sept. 2000.
[79] G. Feher, "Electron spin resonance experiments on donors in silicon. I. Electronic structure of donors by the electron nuclear double resonance technique," *Phys. Rev.*, vol. 114, pp. 1219–1244, June 1959.
[80] E. R. Glaser, T. A. Kennedy, J. A. Freitas, Jr., B. V. Shanabrook, A. E. Wickenden, D. D. Koleske, R. L. Henry, and H. Obloh, "Optically-detected magnetic resonance of shallow donor–shallow acceptor and deep (2.8–3.2 eV) recombination from Mg-doped GaN," *Physica B*, vol. 273/274, pp. 58–62, Dec. 1999.
[81] K. Saarinen, T. Laine, J. Nissilä, P. Hautojärvi, L. Dobrzynski, J. M. Baranowski, K. Pakula, R. Stepniewski, M. Wodjak, A. Wysmolek, T. Suski, M. Leszczynski, I. Grzegory, and S. Porowski, "Observation of native Ga vacancies in GaN by positron annihilation," *Phys. Rev. Lett.*, vol. 79, pp. 3030–3033, Oct. 1997.
[82] J. Neugebauer and C. Van de Walle, "Gallium vacancies and the yellow luminescence in GaN," *Appl. Phys. Lett.*, vol. 69, pp. 503–505, July 1996.
[83] E. R. Glaser, T. A. Kennedy, W. E. Carlos, J. A. Freitas, Jr., A. E. Wickenden, and D. D. Koleske, "Optically detected electron-nuclear double resonance of epitaxial GaN," *Phys. Rev. B*, vol. 57, pp. 8957–8965, Apr. 1998.
[84] G. D. Watkins, private communication.

Robert F. Davis received the Ph.D. degree in materials science and engineering from the University of California, Berkeley, in 1970.

He is a Kobe Steel Ltd. Distinguished University Professor of Materials Science and Engineering with North Carolina State University, Raleigh. His current research interests include growth and characterization of SiC, ZnO, GaN and nitride alloy thin films, the development of lateral and pendeoepitaxial overgrowth, and the deposition and characterization of metallic films on nonmetallic substrates. He has edited or coedited six books, authored or coauthored more than 200 chapters in proceedings or books and more than 300 papers in journals, and given more than 160 invited presentations.

Dr. Davis is a Member of the National Academy of Engineering and the Materials Research Society and a Fellow of the American Ceramic Society. He received the National Collegiate Inventor of the Year Award in 1999, the ALCOA Distinguished Research Award, the ALCOA Award for Research Performance in a Given Year, the Alumni Research Award, the ORNL Excellence in Publications Award, the Richard M. Fulrath Memorial Award from the American Ceramic Society, the R. J. R. Reynolds Award for Excellence in Teaching, Research, and Outreach, and the Alexander Quarles Holladay Medal of Excellence.

Amy M. Roskowski received the B.S. degrees in mechanical engineering and chemistry from Ohio Northern University, Ada, and the Ph.D. degree in chemical engineering from North Carolina State University, Raleigh.

She is currently a Senior Process Engineer with Intel, Portland, OR. Her dissertation research was in the area of MOVPE GaN growth and characterization.

Edward A. Preble received the B.S. degree in mechanical engineering from Worcester Polytechnic Institute, Worcester, MA, and the M.S. degree in in nuclear engineering and the Ph.D. degree in materials science and engineering from North Carolina State University, Raleigh.

He is currently a Post-Doctoral Researcher with the Department of Materials Science and Engineering, North Carolina State University. His dissertation concerned the characterization of III-nitride thin films on SiC substrates.

James S. Speck is a Professor with the Materials Department, University of California, Santa Barbara. His current research interests include the relationship between thin film electronic materials growth, microstructure, and physical properties in compound semiconductors, particularly wide bandgap nitrides and oxide thin films.